

## Spin correlations in the $S = 1$ XXZ chain

Kenn Kubo

*Institute of Physics, University of Tsukuba, Ibaraki 305, Japan*

(Received 30 December 1991; revised manuscript received 27 March 1992)

The spin correlation functions as well as the string correlation functions introduced by den Nijs and Rommelse in the  $S = 1$  XXZ chain have been calculated by using the quantum transfer-matrix method. The temperature variation of the correlation lengths and the susceptibilities has been examined and found to differ according to the phase to which the ground state belongs. The excitation gap is estimated from the temperature dependence of these quantities.

### I. INTRODUCTION

Haldane predicted in 1983 that the antiferromagnetic Heisenberg chain (AFHC) with integer spins has quite different properties from those of the AFHC with half-odd-integer spins.<sup>1</sup> According to his theory, the spin correlations in the ground state decay with a finite correlation length and a finite energy is necessary to excite the system from the ground state in the integer-spin AFHC. Many numerical works as well as theoretical investigations have been performed to check his prediction.<sup>2</sup> After some initial confusion, a general consensus seems to have developed that the predicted ground state (Haldane state) is realized in the  $S = 1$  AFHC. A physical picture of this state has been given by Affleck *et al.*, who constructed the exact ground state of an antiferromagnetic (AF) spin model that contains biquadratic interactions in addition to the usual Heisenberg interaction.<sup>3</sup> They showed rigorously that its ground state—the valence-bond solid (VBS) state—has the properties of the ground state predicted by Haldane. The VBS state is now considered to be a prototype of the Haldane state in the usual AFHC. den Nijs and Rommelse found that the VBS state has a hidden nonlocal order parameter and called it the string-order parameter.<sup>4</sup> They argued that the existence of the string order characterizes the Haldane state. Recently, Kennedy and Tasaki clarified that a full  $Z_2 \times Z_2$  symmetry breaking characterizes the  $S = 1$  Haldane state, which manifests itself in the existence of the long-range string order in all of three spin directions.<sup>5</sup> This was shown to be the case by diagonalizing the finite-size systems.<sup>6</sup>

Most of the numerical works on this problem have concentrated on the study of the ground-state properties of the  $S = 1$  system. So far, little effort has been devoted to the nature of excitations<sup>7</sup> and finite-temperature properties. Kubo and Takada calculated the spin correlations of the  $S = 1$  XXZ chain by making use of the quantum transfer-matrix (QTM) method.<sup>8</sup> They discussed the critical properties at  $T = 0$  by using the QTM with Trotter size up to 6. Finite-temperature correlations were obtained, but not reported in detail. Narayanan and Singh studied the internal energy and specific heat by diagonalizing finite-size systems.<sup>9</sup> They also obtained a correla-

tion length estimated from the cluster expansion. Their correlation length, however, is not that of the spin correlations as we discuss in Sec. IV.

Recently, several materials with  $Ni^{2+}$  ions such as NENP were discovered and their thermodynamic properties were studied.<sup>10</sup> Experiments showed that they realize the Haldane state. So it is worthwhile to examine the finite-temperature properties of the  $S = 1$  AF chains and compare results with experimental ones.

In this paper we investigate the spin correlations in the  $S = 1$  XXZ model at finite temperatures. Though the XXZ model is not directly comparable with real materials, it is interesting to examine how finite-temperature properties differ according to the type of the ground state of the system. The QTM with a Trotter size up to 7 is employed. The usual spin correlations, canonical correlations, and string correlations are examined. From an analysis of the correlation functions, we observe that the temperature dependence of the physical quantities varies with the anisotropy parameter, depending on the type of the realized ground state.

In Sec. II we present the model and associated definitions. The QTM method is briefly explained. In Sec. III numerical results and their analyses are presented. A summary and discussion are given in Sec. IV.

### II. MODEL AND THE METHOD

We investigate the  $S = 1$  XXZ chain with  $2L + 1$  sites described by the Hamiltonian

$$H = \sum_{i=-L}^L (S_i^x S_{i+1}^x + S_i^y S_{i+1}^y + \Delta S_i^z S_{i+1}^z), \quad (1)$$

where  $\Delta$  is the anisotropy parameter of the exchange interactions. We study the spin-correlation functions of the system in the limit of infinite  $L$ . They are defined as

$$f^\alpha(r) = \langle S_0^\alpha S_r^\alpha \rangle \quad (2)$$

and

$$g^\alpha(r) = \int_0^1 dx \langle S_0^\alpha(\beta x) S_r^\alpha \rangle, \quad (3)$$

where  $\langle \dots \rangle$  denotes a thermal average in the infinite system and  $A(\tau) \equiv e^{\tau H} A e^{-\tau H}$ . The former correlation

function is the customary one, and the latter is called a canonical-correlation function, or Duhamel two-point function, and is related to the susceptibility  $\chi_\alpha(q)$  by

$$\chi_\alpha(q) = \frac{3}{2}\beta \sum_{r=-\infty}^{\infty} e^{iqr} g^\alpha(r), \quad (4)$$

which is normalized to be  $\beta^{-1}$  at a high temperature and  $\beta=T^{-1}$ . We also study the string-correlation function introduced by den Nijs and Rommelse, which is given by<sup>4</sup>

$$h^\alpha(r) = - \left\langle S_0^\alpha \exp \left[ i\pi \sum_{i=1}^{r-1} S_i^\alpha \right] S_r^\alpha \right\rangle. \quad (5)$$

It is believed that the  $S=1$  XXZ chain has four different ground-state phases, depending on the value of  $\Delta$ : the ferromagnetic Ising phase at  $\Delta < -1$ ; the XY (or planar) phase at  $-1 < \Delta < \Delta_1$ ; the Haldane phase at  $\Delta_1 < \Delta < \Delta_2$ ; and the Néel (or antiferromagnetic Ising) phase at  $\Delta_2 < \Delta$ . We do not discuss the ferromagnetic Ising phase in this paper. In the XY phase the excitation spectrum is gapless and it is expected that all correlation functions are critical; i.e., they show a power-law decay behavior.<sup>4</sup>

In the Haldane phase,  $f^\alpha(r)$  and  $g^\alpha(r)$  show exponential decay, while  $h^\alpha(r)$  is supposed to approach a finite value as  $r \rightarrow \infty$  for each  $\alpha$ .<sup>5</sup> In the Néel phase, all correlation functions for  $\alpha=z$  oscillate with finite amplitudes as  $r \rightarrow \infty$ , while those for  $\alpha=x$  or  $y$  show exponential decay. The location of the boundary  $\Delta_1$  between the XY and Haldane phases is still not known accurately. It is quite difficult to determine  $\Delta_1$  precisely by numerical methods since the phase transition is of Kosterlitz-Thouless type.<sup>11</sup> On the other hand  $\Delta_2$  is known to be about 1.2.<sup>12</sup>

At finite temperatures all correlation functions decay with finite correlation length regardless of the character of the ground state. We study in the following the temperature dependence of the correlation length and examine how it varies according to the change of the ground state. We also examine the temperature dependence of the susceptibilities.

To obtain thermal averages, we approximate the density matrix as

$$e^{-\beta H} \cong [e^{-\beta H_1/n} e^{-\beta H_2/n}]^n, \quad (6)$$

where  $H_1$  ( $H_2$ ) is the part of the Hamiltonian (1) whose summation runs over only odd (even)  $i$ 's. Let us call the average of an observable  $A$  in this approximation as the  $n$ th approximant of  $A(T)$  and denote it as  $A_n(T)$ . The convergence of the approximant has been verified,<sup>13</sup> and the leading correction is known to be of order  $n^{-2}$ .<sup>14,15</sup> An approximant is expressed in terms of a transfer matrix, i.e., QTM, whose dimension is  $9^n$ . By using some symmetries, one can reduce the size of the matrix. In this work we have used a matrix with  $(9^n+1)/2$  dimensions. The matrix multiplication has been done by using a HITACHI S820 supercomputer. Correlation functions are conveniently calculated by the QTM method as such large systems can be considered to be practically infinite. On the other hand, the Trotter size  $n$  is rather restricted because of the rapid increase of the matrix size. The extrapolation, however, to infinite  $n$  from several approximants with rather modest  $n$ 's is quite effective, as was shown in Ref. 15, and so we can obtain very good estimates of thermal averages at fairly low temperatures. An exact  $A(T)$  is estimated from  $m$  approximants by fitting them to the formula

$$A_n(T) = A(T) + \sum_{l=1}^{m-1} a_l n^{-2l}. \quad (7)$$

We do not extrapolate the approximants of the correlation functions themselves, but those of the correlation length defined by

$$|C(r)| \sim C_0 \varphi(r/\xi) e^{-r/\xi}, \quad (8)$$

where  $C(r)$  represents one of the correlation functions and  $\varphi(x)$  is normalized as  $\lim_{x \rightarrow \infty} \varphi(x) = 1$ . In the XY phase the approximants of the factor  $C_0$  are also extrapolated to yield the correlation index. A detailed explanation of the QTM method can be seen in Ref. 15. In this work extrapolations using the sets of approximants (4,5,6), (5,6,7), (3,4,5,6), and (4,5,6,7) are practiced. Approximants of the correlation length of  $h^z(r)$  for  $\Delta=1$  and the results of the extrapolations from different sets of approximants are shown in Table I. The results of

TABLE I. Correlation length of the string-correlation function  $h^z(r)$  for  $\Delta=1$ .  $\xi_n$ 's ( $n=3, 4, 5, 6$ , and  $7$ ) are the approximants with  $n$  Trotter slicings, and  $\xi_{(n_1, n_2, \dots)}$ 's are the extrapolated values from the approximants with  $n_1, n_2, \dots$  Trotter slicings. The maximum sizes of the calculated systems are also tabulated.

$\beta$	0.5	1.0	2.0	3.2	4.0	5.0	6.4
System size	32	64	72	104	128	176	240
$\xi_3$	0.931 519(1)	1.968 06(1)	5.636 55(2)	12.8597(6)	19.1623(9)	28.5264(6)	45.1050(17)
$\xi_4$	0.931 216(1)	1.964 57(1)	5.617 85(2)	13.0474(7)	19.8998(10)	30.3917(8)	47.9830(21)
$\xi_5$	0.931 074(1)	1.962 86(1)	5.606 54(2)	13.1498(9)	20.4136(9)	32.1755(9)	53.0988(16)
$\xi_6$	0.930 996(1)	1.961 90(1)	5.599 52(1)	13.2061(9)	20.7350(10)	33.4662(14)	57.7743(33)
$\xi_7$	0.930 948(1)	1.961 32(1)	5.594 97(2)	13.2394(8)	20.9403(8)	34.3614(9)	61.4974(64)
$\xi_{(4,5,6)}$	0.930 816(2)	1.959 64(1)	5.581 27(2)	13.3358(1)	21.5762(1)	37.2419(1)	73.3659(2)
$\xi_{(5,6,7)}$	0.930 811(2)	1.959 71(1)	5.581 12(2)	13.3291(1)	21.5540(1)	37.2996(2)	75.3566(5)
$\xi_{(3,4,5,6)}$	0.930 816(2)	1.959 62(1)	5.580 93(2)	13.3291(1)	21.5694(1)	37.3943(2)	75.1193(3)
$\xi_{(4,5,6,7)}$	0.930 809(3)	1.959 74(1)	5.581 05(3)	13.3258(2)	21.5432(2)	37.3276(3)	76.3218(8)

different extrapolations agree quite well at higher temperatures. For lower temperatures they show some disagreement. This difference is still rather small at  $\beta=6.4$ , where the difference between the approximants is appreciable.

We show the mean of two extrapolations from (5,6,7) and (4,5,6,7) as the estimated value at  $n=\infty$  in the following and take half the difference between them as a measure of the error of the estimation, although it is usually too small to be noticeable in the figures. We have made this choice in order to take advantage of the largest Trotter size. Although the errors may be underestimated, we believe that it would not appreciably affect the final results since the difference between results of different extrapolations are still small even at the lowest temperatures examined. We also list the maximum size of the calculated system in Table I. In fact, we have employed a system with  $2M+r-1$  sites to calculate the correlations at distance  $r$ . The same size  $M$  of the margins at both sides of the measured sites is used for different  $r$ 's at a fixed temperature. In the case of Table I,  $M$  is one-quarter of the maximum size. As can be seen from the table,  $M$  is always larger than  $\xi_n$  ( $n=3, 4, 5, 6$ , and  $7$ ) except for  $\beta=6.4$ , where  $M$  is slightly smaller than  $\xi_7$ . We have checked in several cases that if  $M$  is nearly equal to or larger than the correlation length, the calculated correlation functions do not depend on  $M$  up to six digits. So we conclude that our data do not show appreciable finite-size effects even at the lowest temperatures examined.

### III. NUMERICAL RESULTS

The calculation was done at four values of  $\Delta$ , i.e.,  $\Delta=0, 1, 1.1$ , and  $1.4$ . These values were chosen as to represent the  $XY$  phase ( $\Delta=0$ ), Haldane phase ( $\Delta=1$  and  $1.1$ ), and Néel phase ( $\Delta=1.4$ ), respectively. We have calculated  $f^x(r)$  and  $g^x(r)$  for  $1.0 \leq \beta \leq 10.0$  at  $\Delta=0$  and  $1.0 \leq \beta \leq 8.0$  at  $\Delta=1, 1.1$ , and  $1.4$ . For  $h^x(r)$  the region is  $0.1 \leq \beta \leq 5.0$  for  $\Delta=1, 1.1$ , and  $1.4$ . For  $f^z(r)$  and  $h^z(r)$ ,  $0.4 \leq \beta \leq 10.0$  for  $\Delta=0$ ,  $0.4 \leq \beta \leq 6.4$  for  $\Delta=1$ ,  $0.1 \leq \beta \leq 4.0$  for  $\Delta=1.1$ , and  $0.2 \leq \beta \leq 2.5$  for  $\Delta=1.4$ . We have not calculated  $h^x(r)$  for  $\Delta=0$  and  $g^z(r)$  for any  $\Delta$ . We describe the results in the following.

#### A. Correlation functions

The squared inverse correlation length,  $[\xi_x(T)]^{-2}$ , of  $g^x(r)$  is plotted as a function of  $T^2$  in Fig. 1. The figure clearly shows that the  $\xi_x^{-2}(T)$  approaches a finite value as  $T \rightarrow 0$  for  $\Delta=1, 1.1$ , and  $1.4$ , while at  $\Delta=0$  it apparently vanishes at  $T=0$ . At  $\Delta=0$  we obtain, for example,  $\xi_x^{-2}(0) = (1.4 \pm 2.8) \times 10^{-5}$  from a quadratic fit of six data at  $\beta=3.2-10.0$ . Extrapolations from different sets of data give  $\xi_x^{-2}(0)$  of order of  $10^{-4}$ , although the absolute value depends on the data we choose. As the error due to extrapolations are hard to estimate accurately and the obtained  $\xi_x^{-1}(0)$  is so small, we find the result to be consistent with the expectation that  $\xi_x(0) = \infty$ .

At  $\Delta=1$ ,  $\xi_x^{-2}(T)$  shows a linear behavior against  $T^2$  at

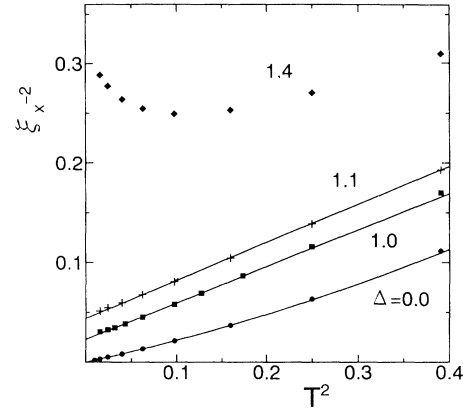


FIG. 1. Squared reciprocal of the correlation length of  $g^x(r)$  is depicted as functions of squared temperature for  $\Delta=0$  (circles),  $1$  (squares),  $1.1$  (crosses), and  $1.4$  (diamonds). Curves show the least-squares fit of seven data values ( $0.1 \leq T \leq 0.4$ ) by a quadratic function of  $T^2$  for  $\Delta=0$ , the seven-point linear fit ( $0.156 \leq T \leq 0.417$ ) for  $\Delta=1$  and the eight-point linear fit ( $0.2 \leq T \leq 1.0$ ) for  $\Delta=1.1$ .

higher temperatures. We obtain  $\xi_x(0) = 6.48(4)$  from a quadratic fit of seven data at  $\beta=2.4-6.4$ . Data at lower temperatures, however, deviate upward from this fit, as can be seen from Fig. 1. It may be more reasonable to assume an exponential dependence on the temperature if the excitation gap exists. We obtain  $\xi_x(0) = 6.1$  by fitting three data for  $\beta \leq 5.6$  to the expression  $\xi_x(T) = \xi_x(0) + CT^{-1}e^{-0.40/T}$ , where we have attached  $T^{-1}$  prefactor to fit the data well, taking the constant of the exponent to be  $0.40$ , which is obtained from the uniform susceptibility. At present stage we cannot determine  $\xi_x(0)$  quite accurately from this calculation. The value  $6.5$  might be considered as an upper bound. Earlier results  $5.5$  (Ref. 16) and  $6.25$  (Ref. 17) obtained by Monte Carlo (MC) simulations are comparable with the present result. We estimate  $\xi_x(0) = 4.65(2)$  for  $\Delta=1.1$  and  $1.77(5)$  for  $\Delta=1.4$ , respectively, from quadratic fits of  $\xi_x^{-2}(T)$  in terms of  $T^2$ . As can be seen from Fig. 1,

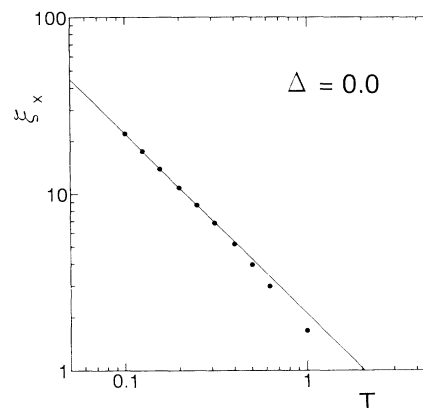


FIG. 2. Log-log plot of  $\xi_x$  vs  $T$  for  $\Delta=0$ . The line shows a least-squares fit of five data values ( $0.1 \leq T \leq 0.25$ ).

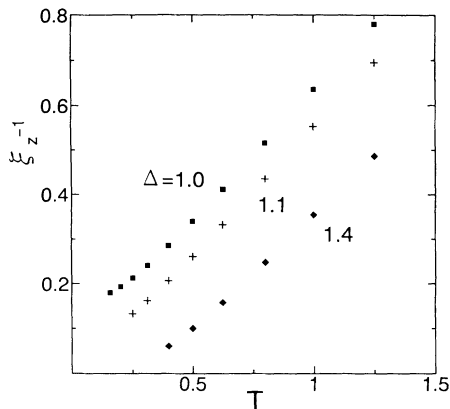


FIG. 3. Inverse correlation length  $\xi_z^{-1}$  of  $f^z(r)$  vs  $T$ .

$\xi_x^{-2}(T)$  shows an interesting temperature dependence at  $\Delta=1.4$ . There occurs a broad minimum at  $T \sim 0.3$ , and  $\xi_x^{-2}(T)$  increases with decreasing  $T$  at lower temperatures.

As a check of the linearity of the data at  $\Delta=0$ , we show  $\ln \xi_x(T)$  plotted against  $\ln T$  in Fig. 2. We estimate  $\nu=1.02$  from data for  $\beta > 4$ , which is consistent with the expectation that  $\nu=1$  throughout the  $XY$  phase.

The inverse of the correlation length  $\xi_z(T)$  of  $f^z(r)$  is shown in Fig. 3 for  $\Delta=1, 1.1$ , and  $1.4$ . At  $\Delta=1.1$ ,  $\xi_z^{-1}(T)$  apparently approaches a small but finite value with decreasing temperature and  $\xi_z(0)$  is estimated as  $17.7(9)$  from a four-point quadratic fit. It is difficult to obtain a more accurate estimate from our data for  $\Delta=1.1$ . At  $\Delta=1.4$ ,  $\xi_z^{-1}(T)$  decrease quite rapidly at low temperatures and seems to vanish at  $T=0$ . The calculation was done only down to  $T=0.4$  in this case as the correlation length of  $g^z(r)$  grows very fast and is estimated to be  $16.3$  at  $T=0.4$ . Data for  $T \lesssim 1$  apparently obey the expression

$$\xi_z(T) = \frac{A}{T} e^{-E_0/T}, \quad (9)$$

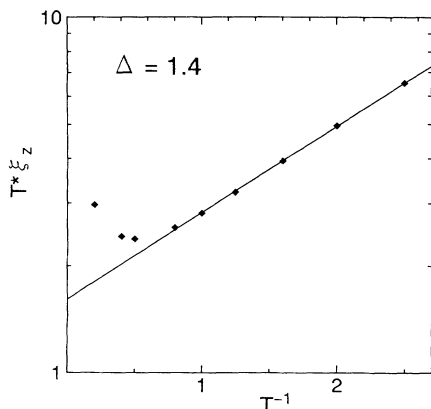


FIG. 4. Logarithmic plot of  $T\xi_z$  vs  $T^{-1}$  for  $\Delta=1.4$ . The line shows a least-squares fit of three data values ( $1.6 \leq T^{-1} \leq 2.5$ ).

as are shown in Fig. 4. We estimate  $A=1.61(5)$  and  $E_0=0.56(1)$  from three data values for  $\beta \geq 1.6$ .

### B. String-correlation functions

In Fig. 5 we show  $\xi_{sz}(T)$  obtained from  $h^z(r)$ . The linear fit with  $T$  of seven data values of  $\xi_{sz}^{-1}(T)$  at  $\Delta=0$  from  $\beta=2.5$  to  $10.0$  leads to  $\xi_{sz}^{-1}(T=0) = -2.5(7) \times 10^{-3}$ . The result seems to be consistent with the divergence of  $\xi_{sz}(T)$  at  $T=0$  as being proportional to  $T^{-1}$ .

For  $\Delta=1, 1.1$ , and  $1.4$ ,  $\xi_{sz}$  increases quite rapidly with decreasing temperature. If we plot  $\ln T \xi_{sz}$  against  $T^{-1}$  as is shown in Fig. 6, we clearly see a linear behavior for  $\Delta=1$  and  $1.1$  at low temperatures. So  $\xi_{sz}$  seems to obey the same temperature dependence as Eq. (9) in the Haldane phase. We estimate  $A=1.46(1)$  and  $E_0=0.326(1)$  from data for  $\beta \geq 2.5$  at  $\Delta=1$  and  $E_0=0.481(3)$  from data for  $\beta \geq 2.0$  at  $\Delta=1.1$ .

Also, at  $\Delta=1.4$  a rapid increase of  $\xi_{sz}$  with decreasing temperature is observed. It is as large as  $45$  at  $\beta=2.5$  and always larger than  $\xi_z$ , which seems consistent with the rigorous relation  $h^\alpha(r) \geq |g^\alpha(r)|$ , which holds for  $\Delta \geq 0$ .<sup>5</sup> As the plot of  $\ln(T^{1/2} \xi_{sz})$  against  $T^{-1}$  shows linear behavior, as is shown in Fig. 7, we suppose that  $\xi_{sz}$  obeys

$$\xi_{sz} = \frac{B}{\sqrt{T}} e^{E_0/T}, \quad (10)$$

with  $B=0.854(3)$  and  $E_0=1.41(1)$ .

In Fig. 8 we show  $\xi_{sx}$  obtained from  $h^x(r)$  at  $\Delta=1.1$  and  $1.4$ . It is clearly seen that  $\xi_{sx}$  diverges at  $T=0$  for  $\Delta=1.1$ , while at  $\Delta=1.4$  it approaches a finite value, which is estimated as  $5.9(2)$ . We fitted data at  $\Delta=1.1$  to Eq. (9) and obtained  $E_0=0.210(5)$  from three data values for  $\beta=3.2-5.0$ . If we choose the power of the prefactor as a fitting parameter, we obtain  $-1.2$  to  $-1.3$  rather than  $-1$  for lower-temperature data. We need further examination at lower temperatures to obtain accurate values of  $E_0$  and the temperature dependence of the prefactor.

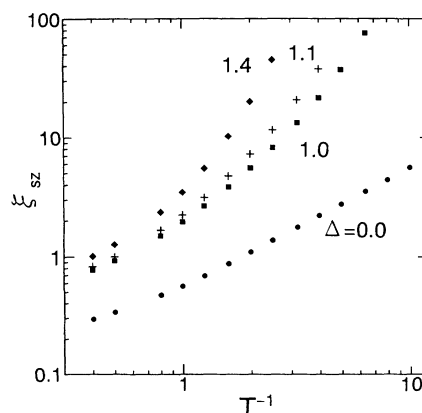


FIG. 5. Log-log plot of the correlation length  $\xi_{sz}$  of  $h^z(r)$  against  $T^{-1}$ .

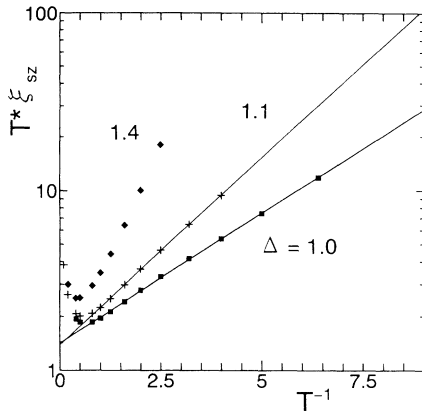


FIG. 6. Logarithmic plot of  $\xi_{sz}$  vs  $T^{-1}$  for  $\Delta=1, 1.1,$  and  $1.4$ . Lines show least-squares fits of nine data values ( $1.0 \leq T^{-1} \leq 6.4$ ) for  $\Delta=1$  and seven data values ( $1.0 \leq T^{-1} \leq 4.0$ ) for  $\Delta=1.1$ , respectively.

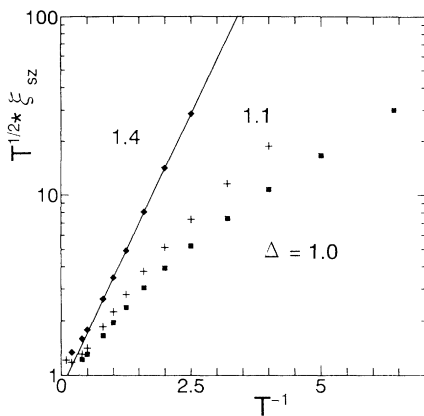


FIG. 7. Logarithmic plot of  $T^{1/2} \xi_{sz}$  vs  $T^{-1}$ . The line shows a least-squares fit of five data values ( $1.0 \leq T^{-1} \leq 2.5$ ) for  $\Delta=1.4$ .

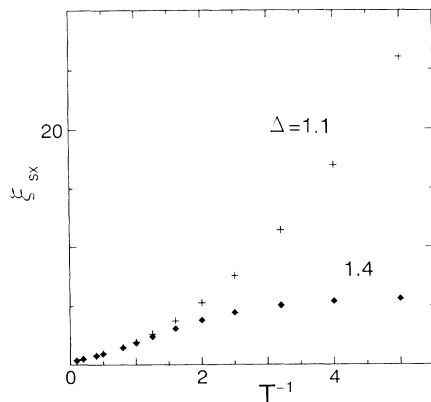


FIG. 8. Correlation length  $\xi_{sx}$  of  $h^x(r)$  vs  $T^{-1}$  for  $\Delta=1.1$  and  $1.4$ .

### C. Susceptibilities

The staggered susceptibility in the  $x$  direction,  $\chi_x(\pi, T)$ , is depicted as a function of temperature in Fig. 9. At  $\Delta=0$ ,  $\chi_x(\pi, T)$  diverges at  $T=0$  while it approaches a finite value for  $\Delta=1, 1.1$  and  $1.4$ . The figure shows an approximately linear behavior of  $\ln \chi_x(\pi, T)$  at  $\Delta=0$  in terms of  $\log T$ . Though data show slight curvature the index  $r$  is estimated to be  $1.80(1)$  from five data for  $\beta=4.0 \sim 10.0$ . At  $\Delta=1$   $\chi_x(\pi, 0)$  is estimated to be  $26.7(1)$  by fitting data to the expression  $\chi_x(\pi, T) = \chi_x(\pi, 0) - Ce^{-E_0/T}$  where we have assumed  $E_0=0.40$  which has been obtained from the analysis of  $\chi_z$ . We just assumed above expression since we have not enough data at low temperatures to deduce a precise temperature dependence. The result is close to the earlier result  $27.6$  obtained by cluster diagonalization.<sup>17</sup> We roughly estimate  $\chi_x(\pi, 0)$  as  $16.4$  and  $2.8$  for  $\Delta=1.1$  and  $1.4$ , respectively. At  $\Delta=1.4$ ,  $\chi_x(\pi, T)$  shows a nonmonotonous temperature dependence.

The uniform susceptibility in the  $z$  direction,  $\chi_z(0, T)$ , is shown in Fig. 10. At  $\Delta=0$ ,  $\chi_z(0, T)$  has a broad peak at  $T \sim 0.7$  and approaches a finite value with decreasing temperature. The value at  $T=0$  is estimated to be  $0.61(1)$ . At  $\Delta=1, 1.1,$  and  $1.4$ ,  $\chi_z(0, T)$  decreases rapidly at low temperatures, indicating the existence of a finite excitation gap. At  $\Delta=1$ ,  $\chi_z(0, T)$  apparently obeys the expression

$$\chi_z(0, T) = DT^{-\epsilon} E^{-E_0/T}, \quad (11)$$

with  $\epsilon = \frac{1}{2}$  as is shown in Fig. 11. From five data values for  $\beta=2.5-6.4$ , we estimate  $D=0.30(1)$  and  $E_0=0.40(1)$ . The obtained value of  $E_0$  is very close to the earlier results of the excitation gap.<sup>18,19</sup> Data at  $\Delta=1.1$  are also plotted in Fig. 11. As is seen from the figure, they are not fitted well by a straight line. If we fit three data values for  $\beta=2.5-4.0$  to Eq. (11) with  $\epsilon = \frac{1}{2}$ , we obtain  $E_0=0.57(1)$ . We obtain a rather small value as  $0.14-0.19$  if we estimate  $\epsilon$  from data for  $\beta=1.25-4.0$ .

At  $\Delta=1.4$   $\chi_z(0, T)$  apparently obeys Eq. (11) with  $\epsilon=1$ , as is also shown in Fig. 11. We estimate  $D=0.78(1)$  and  $E_0=1.56(1)$ .

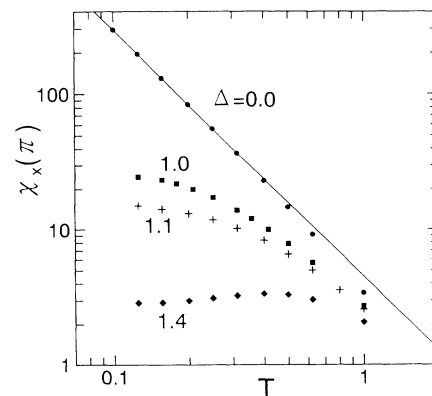


FIG. 9. Log-log plot of the staggered susceptibility in the  $S^x$  direction,  $\chi_x(\pi, T)$  vs  $T$ .

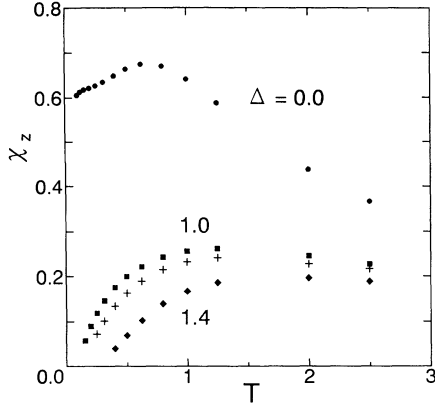


FIG. 10. Uniform susceptibility in the  $S^z$  direction,  $\chi_z(0, T)$  vs  $T$ .

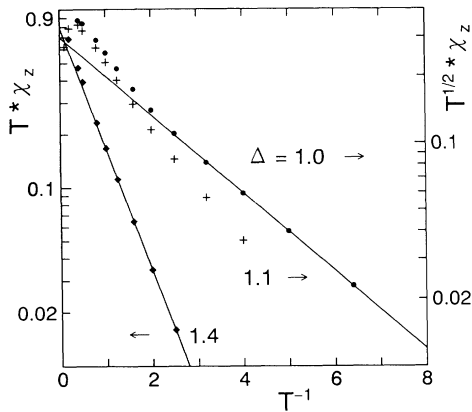


FIG. 11. Logarithmic plot of  $T^{1/2}\chi_z(0, T)$  vs  $T^{-1}$  for  $\Delta=1$  and  $1.1$ .  $\ln[T\chi_z(0, T)]$  is also depicted for  $\Delta=1.4$ . Lines are least-squares fits of five data values ( $2.5 \leq T^{-1} \leq 6.4$ ) for  $\Delta=1$  and that of five data values ( $1.0 \leq T^{-1} \leq 2.5$ ) for  $\Delta=1.4$ , respectively.

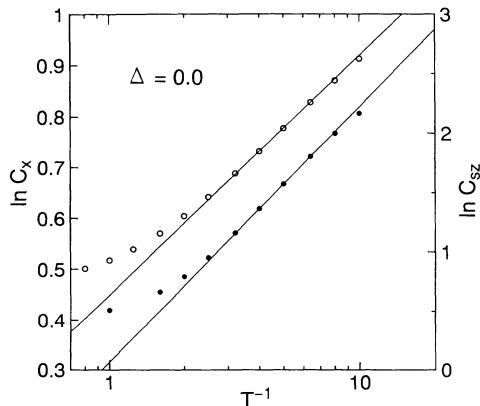


FIG. 12. Log-log plot of  $C_0$  defined in Eq. (8) vs  $T^{-1}$  for  $g^x(r)$  and  $h^z(r)$  at  $\Delta=0$ . Lines show least-squares fits of three data values ( $4.0 \leq T^{-1} \leq 6.4$ ).

#### D. Correlation index

If we assume the scaling property at the ground state,  $C_0$  defined in Eq. (8) diverges as  $C_0 \sim T^{-\nu\eta}$  at low temperatures. The logarithms of  $C_0$  obtained from  $g^x(r)$  and  $h^z(r)$  at  $\Delta=0$  are plotted against  $\ln\beta$  in Fig. 12. The data show approximately linear behavior, although one can observe a slight curvature. The slope first increases with temperature and then decreases at  $\beta \gtrsim 8$ . We estimate  $\eta_x = 0.22(1)$  for the  $S^x$  correlation and  $\eta_{sz} = 0.87(1)$  for the string correlation from data between  $\beta=4.0$  and  $6.4$ .

#### IV. SUMMARY AND DISCUSSION

We have studied the temperature dependence of the correlation length of the spin-correlation functions as well as that of the susceptibilities in the  $S=1$  XXZ chain. These quantities have been calculated by extrapolating approximants with rather a modest number of Trotter slicings (up to 7). We have analyzed the result based on the extrapolations from two sets of approximants (5,6,7) and (4,5,6,7). Although the difference between the result of these extrapolations is less than 4% even at the lowest temperature examined, one cannot exclude the possibility that our results at lowest temperatures may involve errors larger than estimated values. The errors, therefore, quoted in this work should not be interpreted as the expected standard deviation.

The results for  $\Delta=0$  are consistent with the ground state in the XY phase with gapless excitations. The critical index  $\eta_x$  for  $S^x$  correlations is estimated to be 0.22, which is close to but smaller than  $\frac{1}{4}$ , the critical value at  $\Delta=\Delta_1$ . At  $\Delta=\Delta_1$  the correlation length might show a logarithmic dependence on the temperature due to the existence of marginal operators.<sup>20</sup> We have not found any evidence of such behavior. Our result, therefore, is consistent with that  $\Delta_1 > 0$ . This contradicts a recent result by cluster diagonalization.<sup>21</sup> It might be possible, however, that our data are still at not low enough temperatures to observe the possible logarithmic corrections. So it should be quite interesting and desirable to examine the system at much lower temperatures by improving the method.

The results at  $\Delta=1$  are consistent with the fact that the ground state is in the Haldane phase with a finite excitation gap. The gap is evaluated from the temperature dependence of several quantities. The result of the uniform susceptibility leads to the gap of 0.40. On the other hand, the temperature dependence of the string correlation gives a gap energy of 0.33. The former value agrees with earlier calculations very well. In general, it is possible that the low-temperature behaviors of two different quantities are governed by different kinds of excitations with different energy gaps. Excitations such as the AF domain wall may be a candidate which destroys the string order, but does not contribute to the magnetization. We, however, cannot exclude the possibility that the difference obtained here is an artifact due to the lack of data at low enough temperatures. The temperature dependence of the prefactor of the exponential term might be affected by the temperature region employed.

The prefactor should be related to the dispersion relation of the elementary excitations, which should be expressed as

$$\varepsilon(k) \cong E_0 + a_0 k^2, \quad (12)$$

in terms of the wave vector  $k$  of the excitation in the long-wavelength limit. Equation(11) for  $\chi^z(0, T)$  with  $\varepsilon = \frac{1}{2}$  is consistent with this dispersion. We have not examined whether Eq. (10) for the string correlation is consistent with the dispersion (12). The energy region of the elementary excitation described by Eq. (12) might be narrow compared with the temperature studied. Then the temperature dependence of the prefactor may not show a simple power law in this temperature region. It will be affected by the dispersion at larger wave vectors where the dispersion may be quasilinear, as is seen from the result of the MC simulation by Takahashi.<sup>7</sup> So it seems necessary to study still lower temperatures to see whether the present results represent correctly the low-temperature limit.

Results for  $\Delta=1.1$  are also consistent with the Haldane-phase ground state. Especially, the present results show clearly that the ground state has the string order in all spin directions. The result on the excitation gap is also quite interesting. We estimate  $E_0$  as 0.48 and 0.57 from the temperature dependence of  $\xi_{sz}(T)$  and  $\chi^z(0, T)$ , respectively. They are both larger than those for  $\Delta=1$ . On the other hand,  $E_0$  estimated from  $\xi_{sx}(T)$  is 0.21 and smaller than that for  $\Delta=1$ . As has been discussed above,  $E_0$  obtained from  $\chi^z(0, T)$  and  $\xi_{sx}$  may involve considerable errors. The difference between them, however, seems to be too large to regard it as an artifact. So we may conclude that the lowest excitations do not contribute to  $\xi_{sz}(T)$  and  $\chi^z(0, T)$  for  $1 < \Delta < \Delta_2$ . On the other hand, we need further study to conclude whether the  $E_0$ 's obtained from  $\xi_{sz}(T)$  and  $\chi^z(0, T)$  really differ or not.

At  $\Delta=1.4$  the result is consistent with the fact that the ground state is in the Néel phase. Usual spin correlations as well as the string correlations have long-range order in the  $S^z$  direction at  $T=0$ . There is no long-range string order in the  $S^x$  direction. An analysis of the correlation lengths  $\xi_z(T)$  and  $\xi_{sz}(T)$  gives different values of excitation gap as 0.56 and 1.41, respectively. The temperature dependence of the prefactor is also different. The temperature dependence of  $\chi_z(0, T)$  gives a gap of 1.56, which is close to that obtained by  $\xi_{sz}(T)$ . As we have studied the rather high-temperature region for  $\Delta=1.4$ , these results may change if we could study lower temperatures. We have no explanation for these results.

A nonmonotonic temperature dependence of  $\xi_x(T)$  and  $\chi_x(\pi, T)$  is observed at  $\Delta=1.4$ . This feature may be considered to be common in the Néel phase. The reasoning is as follows. The spin correlations at higher temperatures will not exhibit strong anisotropy and therefore increase with decreasing temperature in all spin directions. On the other hand, the ground state has long-range antiferromagnetic order in the  $S^z$  direction and is strongly anisotropic in nature.  $S^x$  correlations there are weak, and the correlation length will be shorter than that in the

TABLE II. Excitation gaps estimated from various quantities are tabulated for  $\Delta=1, 1.1$ , and 1.4. The reciprocals of  $\chi_x(\pi, 0)$ ,  $\xi_x(0)$ ,  $\xi_z(0)$ , and  $\xi_{sx}(0)$  are also tabulated.

$\Delta$	1.0	1.1	1.4
$E_0$ from $\chi_z(0)$	0.40	0.57	1.56
$E_0$ from $\xi_{sz}(T)$	0.33	0.48	1.41
$E_0$ from $\xi_{sx}(T)$	0.33	0.21	
$E_0$ from $\xi_z(T)$			0.56
$[\chi_x(\pi, 0)]^{-1}$	0.036	0.061	0.36
$[\xi_x(0)]^{-1}$	0.15	0.22	0.56
$[\xi_z(0)]^{-1}$	0.15	0.056	
$[\xi_{sx}(0)]^{-1}$			0.17

excited states. At very low temperatures the correlation length will decrease with decreasing temperature as a result of increasing the statistical weight of the ground state. As a result of these two effects there is a nonmonotonic temperature dependence of the  $S^x$  correlations. A similar effect was reported in Monte Carlo simulations of the  $S = \frac{1}{2}$  XXZ chain.<sup>22</sup>

Summarizing our results, we show estimates of the excitation gap as well as the inverse of correlation lengths and  $\chi^x(\pi, 0)$  in Table II. Though we have results at only three values of  $\Delta$ , they suggest that the excitation gaps estimated from  $\xi_{sz}(T)$  and  $\chi_z(0, T)$  increase monotonically with  $\Delta$  across the phase-transition point  $\Delta_2$ . On the other hand, the excitation gap estimated from  $\xi_{sx}(T)$  decreases with  $\Delta$ . We expect that it vanishes at  $\Delta=\Delta_2$ . Also, we expect that the gap estimated from  $\xi_z(T)$  vanishes at  $\Delta=\Delta_2$ . A monotonic increase of  $\xi_x^{-1}(0)$  and  $\chi_x(\pi, 0)^{-1}$  with  $\Delta$  is also seen from the table. A monotonic increase of  $\xi_x^{-1}(0)$  has been reported earlier.<sup>8</sup> At  $\Delta=\Delta_2$ ,  $\xi_{sx}^{-1}(0)$  and  $\xi_z^{-1}(0)$  are expected to vanish. From these results we see that there are two different kinds of excitations which are determining the temperature dependence of correlation functions. We need further study to determine the character of these excitations.

We want to comment here on the correlation length obtained by Narayanan and Singh for  $\Delta=1$ .<sup>9</sup> If we compare their result and ours for  $0.16 < T < 0.2$ , we observe that theirs is much smaller than ours. For example, at  $T=0.2$ , we read from their Fig. 6 that the value is  $\sim 1.3$ , while ours is 5.17. So we conclude that their correlation length is not that of the spin correlations.

In summary, we have obtained a temperature dependence of the correlation functions consistent with the expected ground state for each anisotropy parameter. To obtain a more precise picture of the excitations, we must go beyond the present results and explore their behavior at lower temperatures. We need some further improvements of the method to accomplish this task.

#### ACKNOWLEDGMENTS

The author is grateful to S. Takada, K. Nemoto, and H. Tasaki for useful discussions and comments. This work was supported by a Grant-in-Aid for Scientific research on Priority Areas by the Ministry of Education, Science Culture.

- <sup>1</sup>F. D. M. Haldane, Phys. Lett. **93A**, 464 (1983); Phys. Rev. Lett. **50**, 1153 (1983).
- <sup>2</sup>For a review, see I. Affleck, J. Phys. C **1**, 3047 (1989).
- <sup>3</sup>I. Affleck, T. Kennedy, E. H. Lieb, and H. Tasaki, Phys. Rev. Lett. **59**, 799 (1987); Commun. Math. Phys. **115**, 477 (1988).
- <sup>4</sup>M. den Nijs and K. Rommelse, Phys. Rev. B **49**, 4709 (1989).
- <sup>5</sup>T. Kennedy and H. Tasaki, Phys. Rev. B **45**, 304 (1991); (unpublished).
- <sup>6</sup>S. M. Girvin and D. Arovas, Phys. Scr. T **27**, 156 (1989); Y. Hatsugai and M. Kohmoto, Phys. Rev. B **44**, 1789 (1991).
- <sup>7</sup>M. Takahashi, Phys. Rev. Lett. **62**, 2313 (1989).
- <sup>8</sup>K. Kubo and S. Takada, J. Phys. Soc. Jpn. **55**, 438 (1986).
- <sup>9</sup>R. Narayanan and R. R. P. Singh, Phys. Rev. B **42**, 10 305 (1990).
- <sup>10</sup>J. P. Renard, M. Verdaguer, L. P. Regnault, W. A. C. Erkelens, J. Rossat-Mignod, and W. G. Stirling, Europhys. Lett. **3**, 945 (1987); J. P. Renard, M. Verdaguer, L. P. Regnault, W. A. C. Erkelens, J. Rossamignod, J. Ribas, W. G. Stirling, and C. Vettier J. Appl. Phys. **63**, 3538 (1988); K. Katsumata, H. Hori, T. Takeuchi, M. Date, A. Yamagichi, and J. P. Renard, Phys. Rev. Lett. **63**, 86 (1989); M. Hagiwara, K. Katsumata, I. Affleck, B. I. Halperin, and J. P. Renard, *ibid.* **65**, 3181 (1990).
- <sup>11</sup>A. Luther and D. J. Scalapino, Phys. Rev. B **16**, 1153 (1977); M. den Nijs, Physica **111A**, 273 (1982).
- <sup>12</sup>R. Botet and R. Jullien, Phys. Rev. B **27**, 613 (1983); **28**, 3914 (1983); K. Nomura, *ibid.* **40**, 9142 (1989); T. Sakai and M. Takahashi, J. Phys. Soc. Jpn. **59**, 2688 (1990).
- <sup>13</sup>For a review, see M. Suzuki, in *Quantum Monte Carlo Methods*, edited by M. Suzuki (Springer, Berlin, 1987), p. 2.
- <sup>14</sup>M. Suzuki, Phys. Lett. **113A**, 299 (1985).
- <sup>15</sup>S. Takada and K. Kubo, J. Phys. Soc. Jpn. **55**, 1671 (1986).
- <sup>16</sup>M. Takahashi, Phys. Rev. B **38**, 5188 (1988).
- <sup>17</sup>K. Nomura, Phys. Rev. B **40**, 2421 (1989).
- <sup>18</sup>M. P. Nightingale and H. W. J. Blöte, Phys. Rev. B **33**, 659 (1986).
- <sup>19</sup>T. Sakai and M. Takahashi, Phys. Rev. B **42**, 1090 (1990).
- <sup>20</sup>J. M. Kosterlitz, J. Phys. C **7**, 1046 (1974).
- <sup>21</sup>T. Sakai and M. Takahashi, J. Phys. Soc. Jpn. **59**, 2688 (1990).
- <sup>22</sup>T. Horiki, S. Homma, H. Matsuda, and N. Ogita, Prog. Theor. Phys. **82**, 507 (1989).